Power-dependent Raman scattering in focused geometry

D. A. Cardimona, P. R. Peterson, A. Gavrielides, and L. J. Smellegar
Quantum Optics Branch (AFWL/ARBM), Air Force Weapons Laboratory, Kirtland Air Force Base, Albuquerque, New Mexico 87117
(Received 24 September 1987)

Diffraction and dispersion effects in Raman scattering are investigated, with focused beams and pump depletion. Power broadening and Stark shifting of the molecular energy levels are included in the equations up to second order in intensity (an intermediate-power approximation). The steady-state paraxial wave equation is used to propagate the electric fields which are expanded in a series of rotationally symmetric Gauss-Laguerre functions. These functions allow diffraction and power-dependent effects to be included quite easily with the introduction of a recursive technique used to evaluate the nonlinear coupling coefficients. The resulting equations are solved analytically for a single transverse mode and numerically for the multimode case. Several examples are given for conversion in H_2. In order for the intermediate-power approximation to remain valid, the pump power must be less than 0.015 MW for a beam confocal parameter of 10 cm. Under these conditions we show that power-dependent focusing reduces the Stokes conversion efficiency by a factor of 5 as compared to power-independent focusing.

I. INTRODUCTION

Much of the work in Raman scattering theory has been done assuming collimated geometry, keeping power-dependent effects only to third order in the field and ignoring diffraction. Several approaches to modeling the effects of focusing and/or diffraction in a nonlinear medium have been developed over the years. The simplest extension of the collimated-geometry Raman equations incorporates a geometric beam expansion by allowing the beam radii to be functions of the propagation variable.[1-4] This method may be the simplest, but it is also the least accurate. Another approach is to assume that a single-mode (TEM_{00}), undepleted, Gaussian pump creates a so-called "focused gain" in the Raman-active medium. A "parabolic" approximation, in which the resulting Gaussian gain is approximated by the first two terms of a Taylor expansion of $\exp(-2r^2/W^2)$, renders the paraxial wave equation exactly solvable (for a single-mode Stokes beam).[5-8] This accounts for focusing and diffraction only to the extent that higher-order effects (such as hole burning and annular beam creation) are unimportant. Recently a theory has been developed which keeps the full Gaussian gain and allows the Stokes beam to be generated in as many as 40 Gauss-Laguerre modes.[9-11] This theory is formally analytic; however, it still does not allow for annular pump beams, pump beam hole burning, or pump depletion, in general. A similar mode expansion using Hermite-Gaussian functions has been used to describe diffraction effects in second harmonic generation.[12] In that work, pump depletion was accounted for in an approximate manner by using a perturbative approach.

We have developed a method in which pump depletion can be easily included for rotationally symmetric Raman scattering in a focused configuration. This method relies on a unique recursive technique to evaluate the mode-coupling matrix which arises when Gauss-Laguerre expansions are used for the electric fields. In two previous papers[13] we obtained the coupling matrix Q (see Appendix B) for power-independent depleted-pump Raman scattering, where Q consisted of the integral of a product of four Gauss-Laguerre functions. However, when power-dependent effects are included, the Q matrices must be generalized to more indices. We utilize a generalized recursive technique (described in Appendix B) to calculate these more complex coupling coefficients. This technique can be applied to many problems other than Raman scattering, such as four-wave mixing, self-focusing, and Brillouin scattering. The only restriction is that $P(E)$ be able to be written as a product of powers of the fields. If the problem is not rotationally symmetric, the electric fields may be expanded in a series of Gauss-Hermite functions. The resulting Q matrix is then a product of two integrals, one consisting of $H_i(x)$'s and one consisting of $H_j(y)$'s. A very slight alteration of the method in Appendix B then leads to recursion relations for these integrals over Hermite polynomials.

The saturation effects of the power broadening and Stark shifting of the molecular energy levels[14] can be included by solving the full molecular Bloch equations. Nondiffractive studies of the extra power-dependent terms have very recently been made in the transient[15] and steady-state[16] regimes of stimulated Raman scattering. In this paper, the expanded recursive technique described above is used to study these power-dependent effects in focused geometry. We find that not only is the Stokes gain reduced by the power broadening and Stark shifting, but the natural expansion of the beams due to the focused geometry further reduces the conversion process. The combination of these two effects results in a reduction of the conversion efficiency by a factor of about 5, compared to the efficiency calculated by ignoring the power-dependent effects.

In Sec. II we couple the slowly varying envelope paraxial wave equation to a molecular model which we choose

to be a steady-state far-off-resonance Raman system in H_2. In Sec. III we expand the electric fields in a series of Gauss-Laguerre functions and derive the differential equations for the pump and Stokes expansion coefficients driven by the complete power-dependent polarization. These equations are then written in an intermediate power approximation which is described in detail in Appendix A. At this point it becomes obvious that power broadening reduces the effective Raman gain and Stark shifting introduces additional phase disturbances. The equations are solved analytically for single-mode beams consisting of just the zeroth-order Gaussian mode. The resulting solution shows nicely how power dependence decreases the conversion in focused geometry. In Sec. IV some sample numerical results are provided in order to indicate the power-dependent effects in multimode focused beams. In general, these results agree with the analytic single-mode solution. Finally, Sec. V summarizes the major findings of the paper.

II. RAMAN EQUATIONS

As mentioned in the Introduction, this section is devoted to the coupling between the slowly varying envelope paraxial wave equation and the molecular model. We begin by expanding the electric fields (E_J) and polarizations (P_J) in terms of their steady-state slowly varying envelopes $\mathcal{E}_J$ and $\mathcal{P}_J$ as ($J=s,p$)

$$E_J=\tfrac{1}{2}\hat{\mathbf{e}}\mathcal{E}_J(x,y,z)\exp[i(\omega_j t-k_j z)]+\text{c.c.} , \tag{1a}$$

$$P_J=\tfrac{1}{2}\hat{\mathbf{e}}\mathcal{P}_J(x,y,z)\exp[i(\omega_j t-k_j z)]+\text{c.c.} , \tag{1b}$$

where all the fields are assumed to have the same unit polarization vectors ($\hat{\mathbf{e}}_j=\hat{\mathbf{e}}$). These then are the inputs to the steady-state paraxial wave equation (in cgs units)

$$\nabla_t^2\mathcal{E}_J(x,y,z)-2ik_J\frac{\partial}{\partial z}\mathcal{E}_J(x,y,z)=-4\pi k_J^2\mathcal{P}_J(x,y,z) . \tag{2}$$

We pick a molecular system for which the constants are fairly well characterized, namely, H_2 (see Appendix A). It has been shown that this system displays power-dependent effects in the far-off-resonance regime.[16] The polarization terms $\mathcal{P}_J$ have been derived to be[16]

$$\mathcal{P}_s=\frac{1}{2\pi}\left[\frac{n_1^2(\omega_s)-1}{2}\frac{1-w}{2}+\frac{n_2^2(\omega_s)-1}{2}\frac{1+w}{2}\right]\mathcal{E}_s+\frac{N}{2}\alpha_{12}(\omega_p)q^*\mathcal{E}_p , \tag{3a}$$

$$\mathcal{P}_p=\frac{1}{2\pi}\left[\frac{n_1^2(\omega_p)-1}{2}\frac{1-w}{2}+\frac{n_2^2(\omega_p)-1}{2}\frac{1+w}{2}\right]\mathcal{E}_p+\frac{N}{2}\alpha_{12}(\omega_p)q\mathcal{E}_s . \tag{3b}$$

Here $n_i(\omega)$ is the index of refraction for absorption at frequency ω from the ith molecular state, α_{12} is the off-diagonal component of the material polarizability associated with the two ground vibrational states $|1\rangle$ and $|2\rangle$, and N is the number of molecules/cm^3. Also, w and q are the population inversion and transition amplitude for the two ground vibrational states. These variables satisfy the equations

$$\frac{d}{dt}q+\Gamma q=i\Delta_e q+i\Omega_e^* w , \tag{4a}$$

$$\frac{d}{dt}w+\Gamma_1(w+1)=\frac{i}{2}(\Omega_e q-\Omega_e^* q^*) , \tag{4b}$$

where Γ_1 and 2Γ are the population and coherence decay constants (full width at half maximum). In Eqs. (4) the power-dependent effects are contained in the Stark shift (Δ_e) and the Rabi frequency (Ω_e), which are given by

$$\Delta_e=\frac{1}{4\hbar}\sum_J|\mathcal{E}_J|^2[\alpha_{11}(\omega_J)-\alpha_{22}(\omega_J)] , \tag{5a}$$

$$\Omega_e=\frac{1}{2\hbar}\sum_j\mathcal{E}_J^*\mathcal{E}_{J-1}\alpha_{12}(\omega_J) , \tag{5b}$$

where α_{11} and α_{22} are the diagonal components of the material polarizability associated with states $|1\rangle$ and $|2\rangle$.

In steady state, Eqs. (4) reduce to[16]

$$q_{ss}=\frac{i\Omega_e^*}{\Gamma-i\Delta_e}w_{ss} , \tag{6a}$$

$$w_{ss}=-1+\frac{\Gamma|\Omega_e|^2}{D} , \tag{6b}$$

where $D=\Gamma_1(\Gamma^2+\Delta_e^2)+\Gamma|\Omega_e|^2$. Thus the steady-state field equations take the form

$$\nabla_t^2\mathcal{E}_s(x,y,z)-2ik_s\frac{\partial}{\partial z}\mathcal{E}_s(x,y,z)=-\tfrac{1}{2}k_s^2\left[[n_1^2(\omega_s)-1]\left[2-\frac{\Gamma|\Omega_e|^2}{D}\right]+[n_2^2(\omega_s)-1]\frac{\Gamma|\Omega_e|^2}{D}\right]\mathcal{E}_s-2\pi Nk_s^2\alpha_{12}(\omega_p)\left[\frac{-i\Omega_e}{\Gamma+i\Delta_e}\right]\left[-1+\frac{\Gamma|\Omega_e|^2}{D}\right]\mathcal{E}_p , \tag{7a}$$

$$\nabla_t^2\mathcal{E}_p(x,y,z)-2ik_p\frac{\partial}{\partial z}\mathcal{E}_p(x,y,z)=-\tfrac{1}{2}k_p^2\left[[n_1^2(\omega_p)-1]\left[2-\frac{\Gamma|\Omega_e|^2}{D}\right]+[n_2^2(\omega_p)-1]\frac{\Gamma|\Omega_e|^2}{D}\right]\mathcal{E}_p-2\pi Nk_p^2\alpha_{12}(\omega_p)\left[\frac{i\Omega_e^*}{\Gamma-i\Delta_e}\right]\left[-1+\frac{\Gamma|\Omega_e|^2}{D}\right]\mathcal{E}_s . \tag{7b}$$

These equations have been solved analytically when diffraction is neglected.[16] If we ignore power-dependent broadening and shifting of the molecular energy levels, then all terms of order $|\Omega_e|^2$ should be dropped, yielding the low-power equations prominent in the literature.

III. EXPANSION IN GAUSS-LAGUERRE FUNCTIONS

An efficient way to account for the diffraction of rotationally symmetric beams is to expand the electric field in a series of Gauss-Laguerre functions. These are solutions of the homogeneous paraxial wave equation and are given by[17]

$$U_n(r,z,W)=\frac{1}{W}\sqrt{2/\pi}L_n(2r^2/W^2)\exp\left[-\frac{r^2}{W^2}-i\left[\frac{kr^2}{2R}-(2n+1)\mathrm{Tan}^{-1}(z/z_0)\right]\right] . \tag{8a}$$

Here, $r^2=x^2+y^2$, the L_n's are Laguerre polynomials, $W(z)$ is the beam radius, $R(z)$ is the radius of curvature of the beam wave front, and z_0 is the confocal parameter. These last three quantities satisfy

$$z_0=\tfrac{1}{2}W_0^2k , \tag{8b}$$

$$W^2=W_0^2\left[1+\frac{z^2}{z_0^2}\right] , \tag{8c}$$

and

$$R=z\left[1+\frac{z_0^2}{z^2}\right]=\frac{z_0^2W^2}{zW_0^2} . \tag{8d}$$

The pump and Stokes electric fields are now expanded in a series of Gauss-Laguerre functions as

$$\mathcal{E}_p(r,z)=\sum_n a_{pn}(z)U_n(r,z,W_p)\equiv\sum_n a_{pn}U_{pn} , \tag{9a}$$

$$\mathcal{E}_s(r,z)=\sum_n a_{sn}(z)U_n(r,z,W_s)\equiv\sum_n a_{sn}U_{sn} . \tag{9b}$$

The next step is to substitute these expansions into Eqs. (7) to obtain the differential equations for the expansion coefficients a_{pn} and a_{sn}. Substituting Eq. (9a) into Eq. (7a), multiplying by $U_{s\alpha}^*$, integrating by

$$\int_0^\infty dr\,r\int_0^{2\pi}d\Phi=2\pi\int_0^\infty dr\,r ,$$

and utilizing the orthonormality of the U's results in

$$\frac{d}{dz}a_{s\alpha}=\frac{-\pi}{ik_s}\int_0^\infty r\left\{-\tfrac{1}{2}k_s^2\left[[n_1^2(\omega_s)-1]\left[2-\frac{\Gamma|\Omega_e|^2}{D}\right]+[n_2^2(\omega_s)-1]\frac{\Gamma|\Omega_e|^2}{D}\right]\sum_j a_{sj}U_{sj}\right.$$

$$\left.-2\pi Nk_s^2\alpha_{12}(\omega_p)\left[\frac{-i\Omega_e}{\Gamma+i\Delta_e}\right]\left[-1+\frac{\Gamma|\Omega_e|^2}{D}\right]\sum_\beta a_{p\beta}U_{p\beta}\right\}U_{s\alpha}^*dr \tag{10}$$

for the Stokes amplitudes. The same procedure yields a similar expression for the pump amplitudes. Using the definition of Ω_e and approximating n^2-1 by $2(n-1)$, we obtain the equations for the Stokes and pump amplitudes as

$$\frac{d}{dz}a_{s\alpha}=-ik_s[n_1(\omega_s)-1]a_{s\alpha}-\pi ik_s\Delta n_s\sum_i a_{si}\int_0^\infty rU_{s\alpha}^*U_{si}\frac{\Gamma|\Omega_e|^2}{D}dr+2\pi\omega_s\sum_{\beta,\gamma,\delta}a_{p\beta}a_{p\gamma}^*a_{s\delta}\int_0^\infty rg_pU_{p\gamma}^*U_{s\delta}U_{p\beta}U_{s\alpha}^*\,dr \tag{11a}$$

and

$$\frac{d}{dz}a_{p\alpha}=-ik_p[n_1(\omega_p)-1]a_{p\alpha}-\pi ik_p\Delta n_p\sum_i a_{pi}\int_0^\infty rU_{p\alpha}^*U_{pi}\frac{\Gamma|\Omega_e|^2}{D}dr$$

$$-2\pi\omega_p\sum_{\beta,\gamma,\delta}a_{s\beta}a_{p\gamma}a_{s\delta}^*\int_0^\infty rg_p^*U_{p\gamma}U_{s\delta}^*U_{s\beta}U_{p\alpha}^*\,dr , \tag{11b}$$

where

$$\Delta n_J = n_2(\omega_J) - n_1(\omega_J)$$

and

$$g_p = -w_{ss} N \pi \alpha_{12}^2(\omega_p)/(\Gamma + i\Delta_e) 2\hbar c \ .$$

Equations (11) may now be simplified by making an assumption about the laser powers involved in the scattering process. As they stand, these equations are good for any applied fields. Setting Ω_e and Δ_e equal to zero results in the low-power-limit equations which have already been studied.[13] However, we wish to improve on this approximation. The full equations have Ω_e's and Δ_e's and hence U_n's, in their denominators, which make the integrals intractable. Therefore, we bypass this difficulty by making an intermediate-power approximation (IPA) which keeps terms only up to the order $|\Omega_e|^2/\Gamma_1\Gamma$ and Δ_e/Γ [i.e., we assume $(|\Omega_e|^2/\Gamma_1\Gamma)^2 \ll 1$ and $\Delta_e^2/\Gamma^2 \ll 1$]. It turns out that these approximations are good for intensities up to about 85 MW/cm^2 or a power of about 0.015 MW when $z_0 = 10$ cm (see Appendix A).

We initiate this approximation by separating g_p into its power-dependent and power-independent parts as

$$g_p = \frac{-w_{ss}}{1 + i\Delta_e/\Gamma} g/\omega_s \ , \tag{12a}$$

where

$$g = \frac{N\pi\alpha_{12}^2(\omega_p)}{2\hbar c \Gamma}\omega_s \tag{12b}$$

and is the usual small-signal Raman amplitude gain coefficient.[16] Now by applying the IPA we obtain

$$g_p = \left[1 - \frac{|\Omega_e|^2}{\Gamma_1\Gamma} - i\frac{\Delta_e}{\Gamma}\right] g/\omega_s \ . \tag{12c}$$

Therefore, in the IPA the Stokes expansion coefficients satisfy

$$\begin{aligned}
\frac{d}{dz}a_{s\alpha} = &-ik_s[n_1(\omega_s)-1]a_{s\alpha} - \frac{2ik_s\Delta n_s}{W_s^2}\sum_i a_{si}\exp[i(i\alpha)\mathrm{Tan}^{-1}(z/z_0)] \\
&\times \int_0^\infty dr\, r \frac{|\Omega_e|^2}{\Gamma_1\Gamma} L_i(2r^2/W_s^2)L_\alpha(2r^2/W_s^2)\exp(-2r^2/W_s^2) \\
&+ \frac{8\omega_s}{W_s^2 W_p^2}\pi \sum_{\beta,\gamma,\delta} a_{p\beta}a_{p\gamma}^* a_{s\delta}\exp[2i(-\gamma+\delta+\beta-\alpha)\mathrm{Tan}^{-1}(z/z_0)] \\
&\times \int_0^\infty dr\, r \left[1 - \frac{|\Omega_e|^2}{\Gamma_1\Gamma} - \frac{i\Delta_e}{\Gamma}\right] L_\gamma(2r^2/W_p^2)L_\delta(2r^2/W_s^2)L_\beta(2r^2/W_p^2)L_\alpha(2r^2/W_s^2)\exp(-2r^2/W_s^2 - 2r^2/W_p^2) \ ,
\end{aligned} \tag{13}$$

and the pump expansion coefficients satisfy a similar set of equations. From this equation we see that the Stark shift (Δ_e) merely adds off-resonant dispersion to the free-space propagation phase accumulation $n_1 k_s z$. The effect of the power broadening ($|\Omega_e|^2$) is twofold. It, too, adds some power-dependent phase through the second term, but it also reduces the Stokes gain as is seen in the last term.

Finally, the equations for the Stokes and pump expansion coefficients are

$$\begin{aligned}
\frac{d}{dz}a_{s\alpha} = &-i\{k_s[n_1(\omega_s)-1]a_{s\alpha}\} - i\left[(k_s\Delta n_s\alpha_{12}^2/2\hbar^2\Gamma_1\Gamma)\sum_{i,j,k,l,\beta} a_{s\beta}a_{pi}^* a_{sj}a_{pk}a_{sl}^* C_{ijlk\beta\alpha}^s Q_{jikl\beta\alpha}^s\right] \\
&+ \left[g\sum_{\beta,\gamma,\delta} a_{p\beta}a_{p\gamma}^* a_{s\delta}C_{\alpha\beta\gamma\delta}Q_{\alpha\beta\gamma\delta}\right] - \left[(g/\Gamma_1\Gamma)\sum_{\beta,\gamma,\delta,i,j,k,l} a_{p\beta}a_{p\gamma}^* a_{s\delta}a_{pi}^* a_{sj}a_{pk}a_{sl}^* C_{\alpha\beta\gamma\delta ijkl}Q_{\alpha\beta\gamma\delta\iota jkl}\right] \\
&- i\left[g[\alpha_{11}(\omega_p)-\alpha_{22}(\omega_p)]/\hbar\Gamma\sum_{\beta,\gamma,\delta,i,j} a_{p\beta}a_{p\gamma}^* a_{s\delta}a_{pi}a_{pj}^* C_{\alpha\beta\gamma\delta ij}^p Q_{\alpha\beta\gamma\delta ij}^p\right] \\
&- i\left[g[\alpha_{11}(\omega_s)-\alpha_{22}(\omega_s)]/\hbar\Gamma\sum_{\beta,\gamma,\delta,i,j} a_{p\beta}a_{p\gamma}^* a_{s\delta}a_{si}a_{sj}^* C_{\alpha\beta\gamma\delta\iota j}^s Q_{\alpha\beta\gamma\delta\iota J}^s\right]
\end{aligned} \tag{14a}$$

and

$$\begin{aligned}
\frac{d}{dz}a_{p\alpha} = &-i\{k_p[n_1(\omega_p)-1]a_{p\alpha}\} - i\left[(k_p\Delta n_p\alpha_{12}^2/2\hbar^2\Gamma_1\Gamma)\sum_{i,j,k,l,\beta} a_{p\beta}a_{pi}^* a_{sj}a_{pk}a_{sl}^* C_{ijlk\beta\alpha}^p Q_{jikl\beta\alpha}^p\right] \\
&- \left[\frac{\omega_p}{\omega_s}g\sum_{\beta,\gamma,\delta} a_{s\beta}a_{p\gamma}a_{s\delta}^* C_{\alpha\beta\gamma\delta}Q_{\beta\alpha\gamma\delta}\right] + \left[\left[\frac{\omega_p}{\omega_s}g/\Gamma_1\Gamma\right]\sum_{\beta,\gamma,\delta,i,j,k,l} a_{s\beta}a_{p\gamma}a_{s\delta}^* a_{pi}^* a_{sj}a_{pk}a_{sl}^* C_{\alpha\beta\delta\gamma ijkl}Q_{\beta\alpha\gamma\delta ijkl}\right] \\
&- i\left[\frac{\omega_p}{\omega_s}g[\alpha_{11}(\omega_p)-\alpha_{22}(\omega_p)]/\hbar\Gamma\sum_{\beta,\gamma,\delta,i,j} a_{s\beta}a_{p\gamma}a_{s\delta}^* a_{pi}a_{pj}^* C_{\alpha\beta\delta\gamma ij}^p Q_{\beta\alpha\gamma\delta ij}^p\right] \\
&+ i\left[\frac{\omega_p}{\omega_s}g[\alpha_{11}(\omega_s)-\alpha_{22}(\omega_s)]/\hbar\Gamma\sum_{\beta,\gamma,\delta,i,j} a_{s\beta}a_{p\gamma}a_{s\delta}^* a_{si}a_{sj}^* C_{\alpha\beta\delta\gamma ij}^s Q_{\beta\alpha\gamma\delta ij}^s\right] ,
\end{aligned} \tag{14b}$$

where

$$C_{\alpha\beta\gamma\delta}=\frac{k_p k_s}{(k_p+k_s)\pi z_0(1+z^2/z_0^2)}\exp[-2i(\alpha-\beta+\gamma-\delta)\mathrm{Tan}^{-1}(z/z_0)]\ ,$$

$$C^J_{\alpha\beta\gamma\delta ij}=\frac{k_p k_s k_J}{(k_p+k_s+k_J)4\pi^2 z_0^2(1+z^2/z_0^2)^2}\exp[-2i(\alpha-\beta+\gamma-\delta-i+j)\mathrm{Tan}^{-1}(z/z_0)]\ ,$$

$$C_{\alpha\beta\gamma\delta ijkl}=\frac{\alpha_{12}^2(\omega_p)k_s^2k_p^2}{\hbar^2(k_p+k_s)8\pi^3z_0^3(1+z^2/z_0^2)^3}\exp[-2i(\alpha-\beta+\gamma-\delta+i-j+k-l)\mathrm{Tan}^{-1}(z/z_0)]\ ,$$

$$Q_{\alpha\beta\gamma\delta}=\int_0^\infty e^{-x}L_\alpha\left[\frac{k_s}{k_s+k_p}x\right]L_\beta\left[\frac{k_p}{k_s+k_p}x\right]L_\gamma\left[\frac{k_p}{k_s+k_p}x\right]L_\delta\left[\frac{k_s}{k_s+k_p}x\right]dx\ ,$$

$$Q^J_{\alpha\beta\gamma\delta ij}=\int_0^\infty e^{-x}L_\alpha\left[\frac{k_s}{k_s+k_p+k_J}x\right]L_\beta\left[\frac{k_p}{k_s+k_p+k_J}x\right]L_\gamma\left[\frac{k_p}{k_s+k_p+k_J}x\right]L_\delta\left[\frac{k_s}{k_s+k_p+k_J}x\right]$$
$$\times L_i\left[\frac{k_J}{k_s+k_p+k_J}x\right]L_j\left[\frac{k_J}{k_s+k_p+k_J}x\right]dx\ ,$$

$$Q_{\alpha\beta\gamma\delta ijkl}=\int_0^\infty e^{-x}L_\alpha\left[\frac{k_s/2}{k_s+k_p}x\right]L_\beta\left[\frac{k_p}{k_s+k_p}x\right]L_\gamma\left[\frac{k_p}{k_s+k_p}x\right]L_\delta\left[\frac{k_s}{k_s+k_p}x\right]$$
$$\times L_i\left[\frac{k_p}{k_s+k_p}x\right]L_j\left[\frac{k_s}{k_s+k_p}x\right]L_k\left[\frac{k_p}{k_s+k_p}x\right]L_l\left[\frac{k_s}{k_s+k_p}x\right]dx\ .$$

These equations contain complicated integrals of products of Laguerre polynomials which can be solved without resorting to numerical integration. This analytic technique, developed in Appendix B, yields a set of recursion relations for the Q integrals which in turn can be manipulated extremely rapidly by computer. Before proceeding we wish to mention that in the above development we assume that the two beams have the same confocal parameter z_0. This assumption allows the Q's to be written as z-independent quantities. Also, in the IPA the photon number is conserved and takes the form $|a_s|^2/\omega_s+|a_p|^2/\omega_p=\text{const}$, where $|a_s|^2=\sum_\alpha|a_{s\alpha}|^2$.

In order to gain some analytical insight into the power-dependent problem, we now consider the case in which the pump and Stokes beams are single Gauss-Laguerre modes. In particular, we estimate the effects that focusing and high powers have on reducing the Stokes conversion. If only the zeroth-order mode is allowed and the new variables $\eta\equiv|a_s|^2/\omega_s+|a_p|^2/\omega_p$ and $\zeta\equiv|a_s|^2/\omega_s-|a_p|^2/\omega_p$ are introduced, Eqs. (11) in the IPA yield $d\eta/dz=0$ and

$$\frac{d\zeta}{dz}=\frac{2g\omega_p}{\pi(W_{s0}^2+W_{p0}^2)(1+z^2/z_0^2)}[1-(\eta^2-\zeta^2)/B]\times(\eta^2-\zeta^2)\ , \tag{15}$$

where

$$B=\frac{\pi^2W_{s0}^2W_{p0}^2\,8\hbar^2\Gamma_1\Gamma}{\omega_s\omega_p\alpha_{12}^2(\omega_p)}\ .$$

Here B has been approximated as a z-independent quantity by letting $W_J^2(z)=W_{J0}^2$ $(J=p,s)$. This should not have much of an effect on the total z dependence of the final solution since the term we are approximating is the small power-dependent part. With this minor approximation, Eq. (15) can be integrated to give

$$\ln\left|\frac{a_{s0}a_p(z)}{a_{p0}a_s(z)}\right|^2-\frac{2\eta}{(\beta-\eta^2)^{1/2}}\left[\mathrm{Tan}^{-1}\left[\frac{\zeta}{(B-\eta^2)^{1/2}}\right]-\mathrm{Tan}^{-1}\left[\frac{\zeta_0}{(B-\eta^2)^{1/2}}\right]\right]$$
$$=\left|\frac{a_{s0}a_p(z)}{a_{p0}a_s(z)}\right|^2-2\eta(\zeta-\zeta_0)/B=-2gI_0z_0\Delta\Theta\ , \tag{16}$$

where $\eta^2/B=\zeta_{\max}^2/B=\frac{1}{2}|\Omega_e|^2_{\max}/\Gamma_1\Gamma$ (see Appendix A) and we have used the IPA to drop terms smaller than $|\Omega_e|^2/\Gamma_1\Gamma$,

$$I_0=\frac{2\omega_p\eta}{\pi(W_{s0}^2+W_{p0}^2)}=\frac{[(8\pi/c)\times10^{13}]2}{\pi(W_{s0}^2+W_{p0}^2)}P_{p0}$$
$$=\frac{(8\pi/c)\times10^{13}}{1+\omega_p/\omega_s}I_{p0}\ ,$$

and

$$\Delta\Theta=\mathrm{Tan}^{-1}(z/z_0)-\mathrm{Tan}^{-1}(z_{in}/z_0)\ .$$

Equation (16) can be rewritten in a form analogous to the single-mode plane-wave case as

$$\left|\frac{a_s(z)}{a_{s0}}\right|^2=\frac{\left[1+\frac{\omega_p}{\omega_s}\left|\frac{a_{s0}}{a_{p0}}\right|^2\right]\exp(2g'I_0z_0\Delta\Theta)}{1+\frac{\omega_p}{\omega_s}\left|\frac{a_{s0}}{a_{p0}}\right|^2\exp(2g'I_0z_0\Delta\Theta)}\ , \tag{17}$$

where the power-dependent effective gain is

$$g'=g\frac{\eta(\zeta-\zeta_0)}{BI_0z_0\Delta\Theta}\ ,$$

which equals $0.85g$ for $\omega_p=\omega_s$, $z_0=10$ cm, $z=-z_{\mathrm{in}}=L/2=50$ cm, and $I_s(z)=I_{p0}=50$ MW/cm^2.

The increase in z at which a specific Stokes power occurs, due to the lower gain, can now be determined by solving Eq. (16) for z. This gives

$$z=z_0\tan\left[\frac{\ln\left[\frac{P_{p0}P_s}{P_{s0}P_p}\right]+2\eta[(8\pi/c)\times10^{13}]\left[2\frac{P_s}{\omega_s}+\frac{P_{p0}}{\omega_p}\right]/B}{2gI_0z_0}+\mathrm{Tan}^{-1}(z_{\mathrm{in}}/z_0)\right]\ , \tag{18}$$

where P is the power in MW, i.e., $P=[(c/8\pi)\times10^{-13}]\,|\,\mathcal{E}\,|^2$. We first calculate $(z-z_{\mathrm{in}})$ in both the intermediate-power and low-power limits and then take the difference between the two to be $\Delta z(z_0)$, with the result that

$$\Delta z(z_0)=z_0\left[\tan\left[\frac{\Delta z(\infty)}{z_0}+\frac{\Delta z_{LP}}{z_0}\right]-\tan\left[\frac{\Delta z_{LP}}{z_0}\right]\right]\ , \tag{19a}$$

where

$$\Delta z(\infty)=\frac{\alpha_{12}[(8\pi/c)\times10^{13}]2}{2g\,8\hbar^2\Gamma_1\Gamma\pi W_{p0}^2}(2P_s-P_{s0})$$

$$=(0.0936)\frac{2}{\pi W_{p0}^2}P_s=(0.0936)\frac{\omega_p}{\omega_s}I_s\ , \tag{19b}$$

$$\Delta z_{LP}=\frac{\ln\left[\frac{P_{p0}P_s}{P_{s0}P_p}\right]}{2gI_0}+z_0\tan^{-1}(z_{\mathrm{in}}/z_0) \tag{19c}$$

and $z_0=\infty$ is the plane-wave result. The plane-wave interaction length increase $\Delta z(\infty)$ corresponds to Eq. (21) of Ref. 16. Because of the expanding geometry and the corresponding reduction in intensity in Gaussian beam propagation, there is a limit to the possible Stokes output power depending on the initial P_{p0}/P_{s0} ratio and z_0. Therefore, using a small signal intensity gain G of 0.008 cm/MW with $2g=[(c/8\pi)\times10^{-13}]G$ and carefully choosing appropriate values of $P_{p0}=0.015$ MW, $P_{p0}/P_{s0}=10^5$, and $P_s(z_{\mathrm{out}})=0.04P_{p0}$ for $z_{\mathrm{in}}=-50$ cm, we find $\Delta z(1\text{ cm})=0.226$ cm, $\Delta z(10\text{ cm})=4.75$ cm, and $\Delta z(100\text{ cm})=0.991$ cm. Note that in this constant-power case, $\Delta z\to0$ as $z_0\to\infty$ since $I\to0$ as $z_0\to\infty$ and the power-dependent effects vanish. If, on the other hand, we keep the input pump intensity constant (allowing the power to vary as z_0 is varied) at $I_{p0}=85$ MW/cm^2 (corresponding to $P_{p0}=0.015$ MW for $z_0=10$ cm) and use $I_{p0}/I_{s0}=10^5\lambda_s/\lambda_p$ and $I_s(z_{\mathrm{out}})=0.04\ I_{p0}\lambda_s/\lambda_p$, then $\Delta z(1\text{ cm})=0.327$ cm, $\Delta z(10\text{ cm})=4.75$ cm, and $\Delta z(100\text{ cm})=0.331$ cm [with $\Delta z(\infty)=0.318$ cm for these parameters].

The reason Gaussian beams exhibit a larger holdoff in power-dependent conversion than plane-wave beams is simple. The lower gain causes the Stokes conversion to be held off in both cases, but as the Gaussian beam propagates the intensity decreases as it diffracts and expands. So, not only do Gaussian beams get a late start in the conversion to Stokes light, but that conversion process is cut short due to a lower diffracted intensity.

We close this section with a brief description of the numerical procedure involved in the solution of Eqs. (14). First notice that the Q's are independent of z because all the beams have the same z_0. Thus the Q matrices are generated external to the differential equation solver and the elements are accessed as needed. The differential equation subroutine consists of Eqs. (14a) and (14b). These are then, in turn, solved for the amplitudes $a_{s\alpha}, a_{p\alpha}$ with a predictor-corrector integration routine in the International Math and Statistics Library.

IV. EXAMPLES

For illustrative purposes, we use a confocal parameter of $z_0=10$ cm, a Raman cell length of $L=100$ cm, and a Stokes small-signal intensity gain coefficient of $G=0.008$ cm/MW ($G=2g[(8\pi/c)\times10^{13}]$). As mentioned before, the Raman medium is H_2 and all the relevant molecular parameters, as well as the pump and Stokes wavelengths, are listed in Appendix A.

As a matter of practical importance we deliberately keep the extraction efficiency under 25%, thus eliminating the generation of higher-order Raman processes. With this restriction we find that four Gauss-Laguerre modes are adequate. That is, the amplitude of mode 0 is about an order of magnitude larger than that of mode 3, which indicates good convergence and a well-established radial profile. Finally, in all of the simulations, power is conserved to better than 0.05%. The moderate conversion efficiency of 25% has two other implications. First,

the input power has to be restricted to less than 0.015 MW (see Appendix A). Second, the radial intensity profiles do not spread very much. In fact, because of the lowered extraction, there is less spreading in the IPA than in the low-power case and hence the IPA radial profiles resemble free-space propagation. Therefore, we only show plots of the Stokes power buildup versus z to indicate the differences between the low-power approximation (solid curves) and the intermediate-power approximation (dashed curves). In all cases, we take the Stokes seed to have a power 10^{-5} that of the input pump. For the parameters used in these examples, the nonlinear Raman interaction does not become important until very near the focus at $z=0$. Soon thereafter the intermediate-power-limit curves become distinctly different from the low-power-limit curves due to the reduction in the power-dependent gain. After the focal spot, Gaussian propagation causes the beams to expand with a corresponding decrease in on-axis intensity, thereby forcing the nonlinear Raman scattering process back into significance.

In Fig. 1, the input pump is a zeroth-order Gaussian,

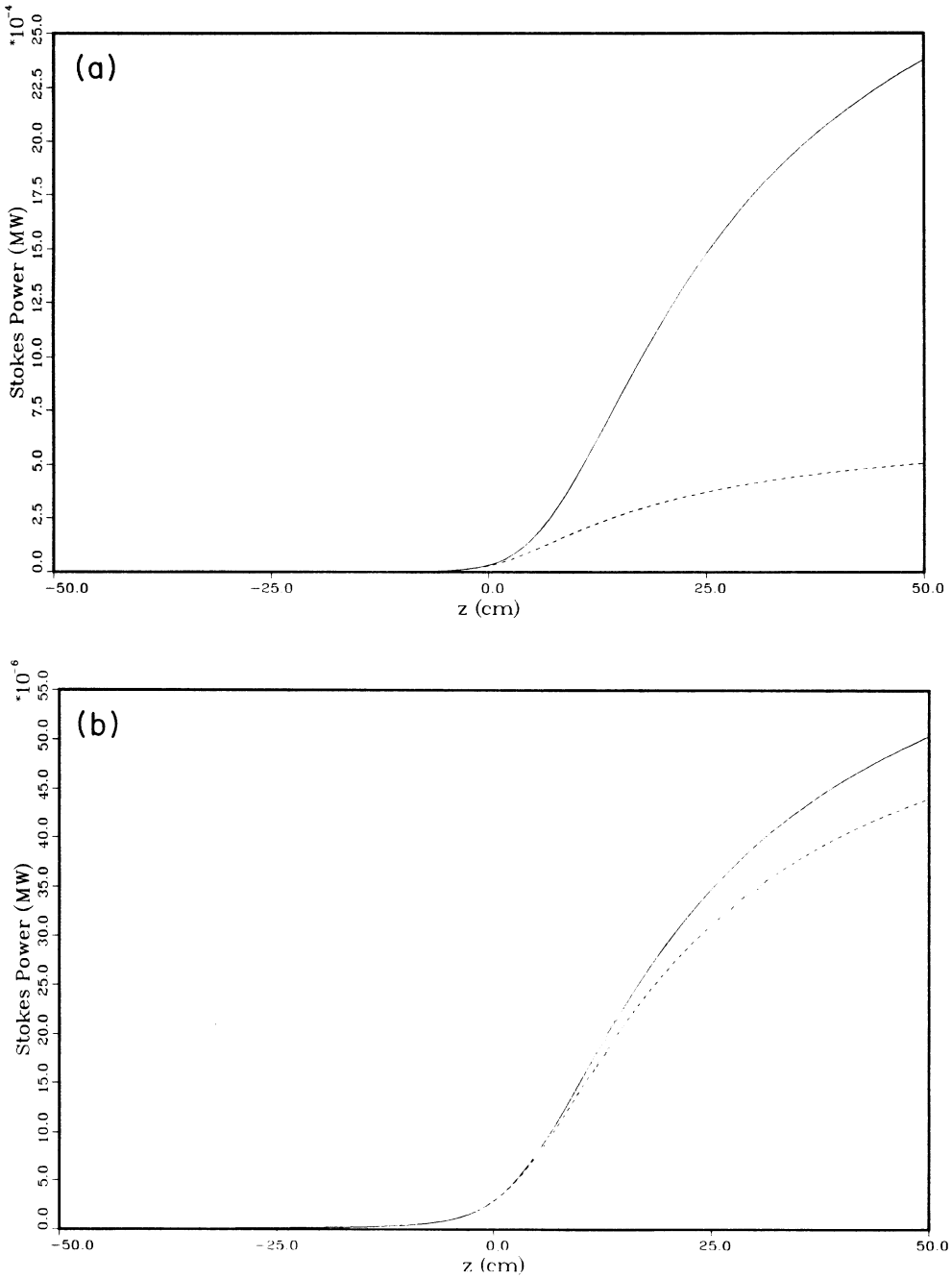

FIG. 1. Stokes power vs z for input pump powers of (a) 0.015 MW and (b) 0.01 MW. Both the pump and Stokes input radial profiles are Gaussian. The solid curve arises from the low-power approximation and the dashed curve from the intermediate-power approximation.

as is the Stokes seed. Figure 1(a) has an input pump power of 0.015 MW which results in a conversion efficiency, equal to

$$(P_s/\omega_s)/(P_{p0}/\omega_p + P_{s0}/\omega_s) \approx P_s\omega_p/P_{p0}\omega_s$$

of 19% in the low-power limit and only 4% in the intermediate-power limit. This corresponds to a reduction by a factor of nearly 5 in efficiency when power-dependent effects are accounted for. The input power for Fig. 1(b) is 0.01 MW. In this case, the conversion efficiencies with and without the power-dependent terms are very nearly the same at 0.52% and 0.59%, respectively. The low-power conversion efficiencies of 19% and 0.52% are consistent with the very reasonable undepleted exponential gIL product of 7. In Fig. 2, both the input pump and the Stokes seed are annular (equal and opposite amplitudes in the zeroth and first modes at $z = -50$ cm). The on-axis focal intensity is higher for the annular input than for the Gaussian input, so the low-power limit

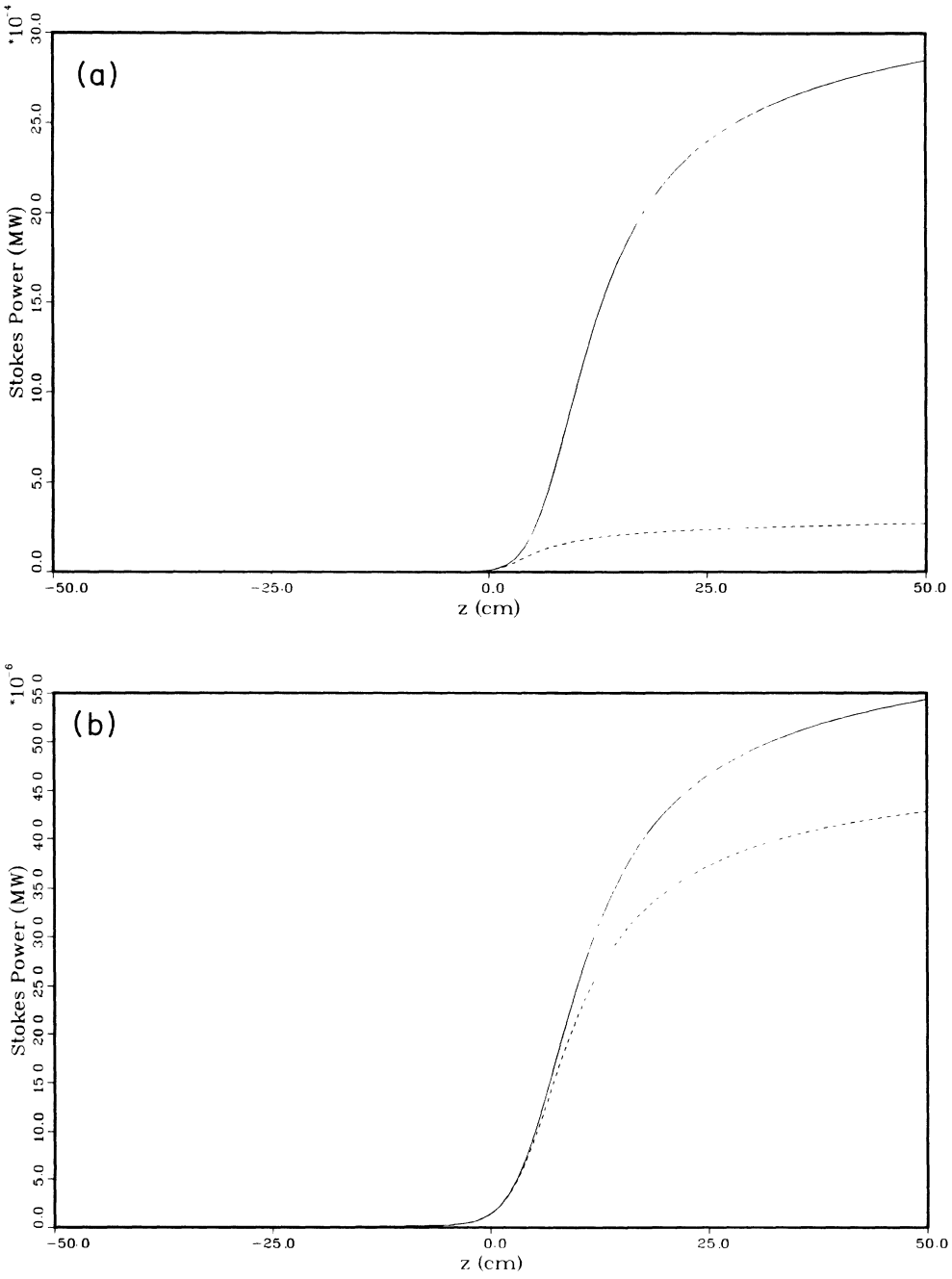

FIG. 2. Stokes power vs z for input pump powers of (a) 0.015 MW and (b) 0.01 MW. Both the pump and Stokes input radial profiles are annular (equal amplitudes, both opposite signs in the zeroth and first Gauss-Laguerre modes). The solid curve arises from the low-power approximation and the dashed curve from the intermediate-power approximation.

conversion efficiency is larger, while the intermediate-power limit efficiencies are lower since the power-dependent terms kept in that limit have a greater effect. In Fig. 2(a), with an input pump power of 0.015 MW, the extraction for the low- and intermediate-power approximations are 22% and 2%, respectively. The conversion efficiencies for Fig. 2(b) with an input pump power of 0.01 MW are 0.64% and 0.5% for the low- and intermediate-power limits. The input pump beam in Fig. 3 is a single-mode Gaussian, as in Fig, 1; however, the Stokes seed beam is given equal amplitudes in the first four Gauss-Laguerre modes. Because the initial Stokes spectrum is flat and since the pump interacts most strongly with the zeroth mode, the pump-Stokes overlap is not very great. Accordingly, the resulting conversion efficiencies are much smaller. For an input pump power of 0.015 MW [Fig. 3(a)], the conversion efficiencies are 9% and 3% in the low- and intermediate-power approximations, respectively. With a pump input of 0.01 MW [Fig. 3(b)], the efficiencies are much closer at 0.19% and 0.18%.

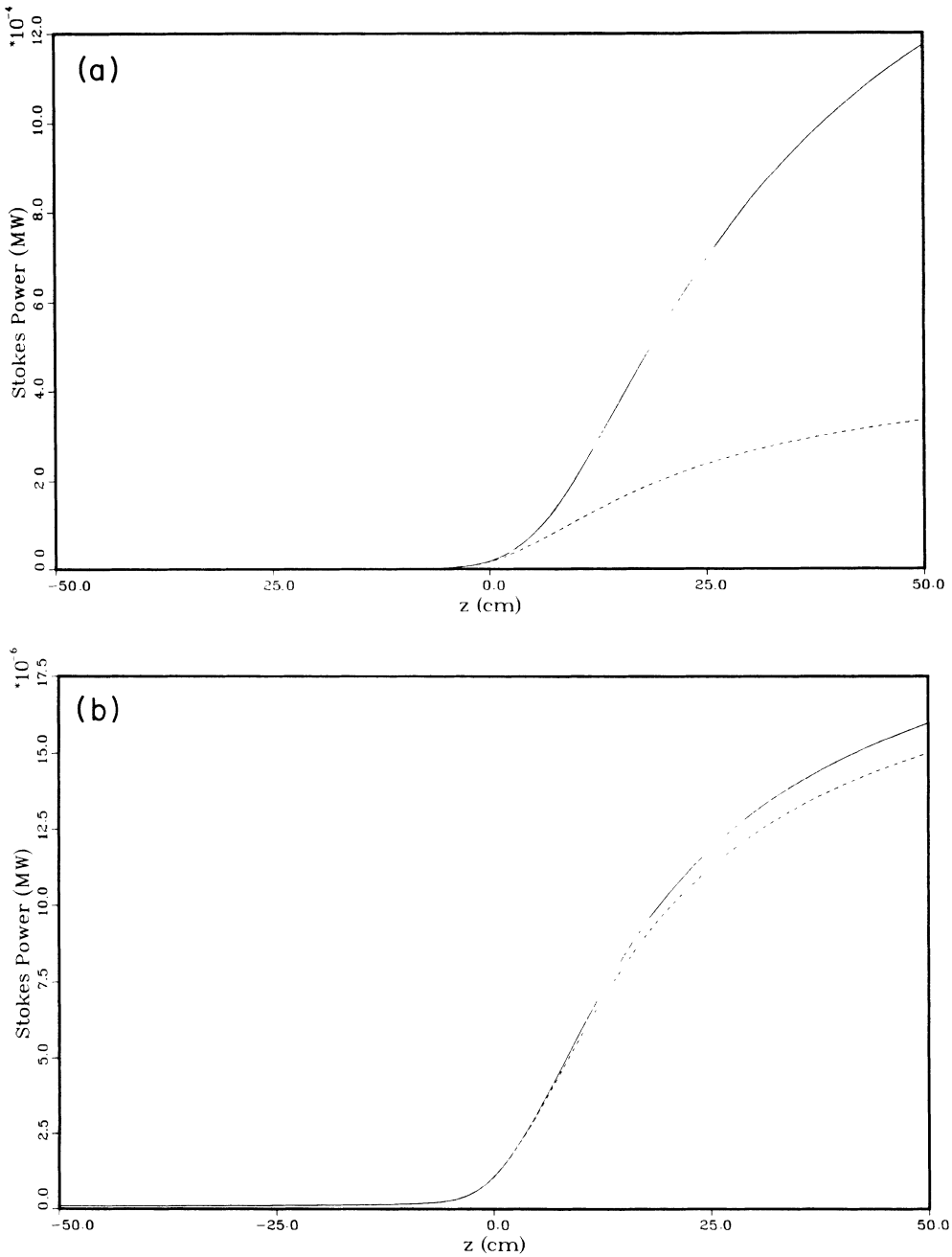

FIG. 3. Stokes power vs z for input pump powers of (a) 0.015 MW and (b) 0.01 MW. Here the pump input radial profile is a Gaussian, while the Stokes input has equal amplitudes in the first four Gauss-Laguerre modes. The solid curve arises from the low-power approximation and the dashed curve from the intermediate-power approximation.

V. SUMMARY

We have solved the steady-state power-dependent Raman scattering equations with depleted pump in focused, rotationally symmetric geometry in an intermediate-power approximation. The IPA is defined by dropping terms of order $(|\Omega_e|^2/\Gamma_1\Gamma)^2$ and $(\Delta_e/\Gamma)^2$ (see Appendix A), where Ω_e is the generalized Rabi frequency, Δ_e is the Stark shift, and Γ_1 and 2Γ are the population and coherence decay constants, respectively. The paraxial wave equation determined the propagation and the fields were represented by an expansion in Gauss-Laguerre functions. Finally, the solution was expedited by the development of a recursive technique used to evaluate the mode coupling coefficients.

We found that the extraction efficiency in power-dependent focused geometry is much less than the low-power plane-wave conversion for two reasons. First, high powers produce power-dependent broadening and shifting of the molecular energy levels which decrease the gain and hold off the Stokes conversion. Second, the focused geometry causes the conversion to begin very near the beam waist, reducing the effective gain length. Thus, just as the power-dependent gain begins to convert pump to Stokes, the bean geometry expands and conversion does not become as well established as it does in the plane-wave case. These conclusions were verified by multimode computer simulations, as well as being evident in a single-mode IPA analytic solution. Our examples modeled Stokes conversion in a 100-cm-long cell of H_2 at 10 atm with pump and Stokes confocal parameters each equal to 10 cm. For an input pump power of 0.015 MW and a z_0 of 10 cm, the single-mode analytic result indicates that to reach the point where the Stokes intensity is about 4% of the input pump intensity with the power-reduced gain in the plane-wave case [Eq. (19b)] requires about 0.3 cm more interaction length than would be needed if the power-dependent effects were ignored. The focused geometry case requires nearly 5 cm more gain length [Eq. (19a)]. Using four Gauss-Laguerre modes in the numerical simulation, we found that the Stokes conversion efficiency was reduced by as much as a factor of 5 when power-dependent effects were accounted for.

The IPA in H_2 requires that the input pump power not exceed 0.015 MW. In this power regime, four Gauss-Laguerre modes were sufficient. If we had run much closer to threshold or well beyond full pump depletion, more than four modes would have been required to adequately describe the radial development. Regardless of the number of modes used, however, the recursive technique described in Appendix B for evaluating the Q-integral coupling constants is extremely efficient. At a power of 0.015 MW, the low-power-limit conversion efficiencies were kept below 20% and the intermediate-power-limit efficiencies never rose above 4%. Even in this relatively low-power regime, the gain-reducing effects of power broadening and Stark shifting have very pronounced effects on the Stokes conversion in focused geometry. Thus, the focused power-dependent effects should be observable without the added complication of higher-order Stokes scattering.

APPENDIX A: INTERMEDIATE POWER APPROXIMATION

The intermediate power approximation is determined using the following constants for Raman scattering in H_2 at 10 atm:

$$\omega_p = 5.34\times10^{15}/\text{sec}$$

(353 nm),

$$\omega_s = 4.56\times10^{15}/\text{sec}$$

(414 nm),

$$N = 2.68\times10^{20}/\text{cm}^3 ,$$

$$\Gamma = 550\times10^{6}/\text{sec}$$

(Ref. 18),

$$\Gamma_1 = 53.6\pi\times10^{3}/\text{sec}$$

(Ref. 19),

$$\alpha_{11}(\omega_p) = 8.63\times10^{-25}\ \text{cm}^3 ,$$

$$\alpha_{22}(\omega_p) = 9.42\times10^{-25}\ \text{cm}^3 ,$$

$$\alpha_{12}(\omega_p) = 1.17\times10^{-25}\ \text{cm}^3$$

(Ref. 20). Using the definition of Δ_e [Eq. (5a)], we find the maximum Stark shift to be in the first half of the cell when $\mathcal{E}_p = \mathcal{E}_{p0}$ and $\mathcal{E}_s = 0$, which gives

$$|\Delta_e|_{\max} = \frac{1}{4\hbar}|\mathcal{E}_{p0}|^2|\alpha_{11}(\omega_p)-\alpha_{22}(\omega_p)| . \quad \text{(A1)}$$

With $|\mathcal{E}|^2 = (8\pi/c)\times10^7\ (\text{erg/J})\times10^6\ (\text{W/MW})\ I$, I equal to the number of MW/cm^2, we find

$$|\Delta_e| < 1.6\times10^5 I_{p0}/\text{sec} . \quad \text{(A2)}$$

Similarly, using the definition of Ω_e [Eq. (5b)], we find that the maximum Rabi frequency occurs when $\mathcal{E}_s = \sqrt{\omega_s/\omega_p}\,\mathcal{E}_{p0}/\sqrt{2}$. This gives

$$|\Omega_e|_{\max} = \frac{1}{2\hbar}\left[\frac{\omega_s}{\omega_p}\right]^{1/2}\tfrac{1}{2}|\mathcal{E}_{p0}|^2\alpha_{12}(\omega_p) . \quad \text{(A3)}$$

Again with the definition of I_{p0} equal to the number of input pump MW/cm^2, the above becomes

$$|\Omega_e| < 2.1\times10^5 I_{p0}/\text{sec} . \quad \text{(A4)}$$

For the zeroth-order approximation in which terms only to third order in the $\mathcal{E}$'s are kept, we require

$$\frac{|\Omega_e|^2}{\Gamma_1\Gamma} , \frac{|\Delta_e|}{\Gamma} < 10^{-1} , \quad \text{(A5)}$$

which therefore limit I_{p0} to be less than 25 MW/cm^2. For the second-order, intermediate-power approximation used in this paper, we require

$$\left[\frac{|\Omega_e|^2}{\Gamma_1\Gamma}\right]^2 , \left[\frac{\Delta_e}{\Gamma}\right]^2 < 10^{-1} , \quad \text{(A6)}$$

which limits I_{p0} to be less than 85 MW/cm^2. By using

$I=2P/\pi W^2=2P/\lambda z_0$, this maximum input intensity converts to a power of about 0.015 MW for $z_0=10$ cm.

APPENDIX B: DETERMINATION OF THE Q INTEGRALS

The Q coupling constants in Eqs. (14) are complicated integrals of products of Laguerre polynomials. They can, of course, be evaluated by brute-force numerical integration. However, a much more efficient procedure was introduced in Ref. 13. In this appendix, we extend this method to the evaluation of integrals over any number of Laguerre polynomials.

The generic Q integral can be written as

$$Q_{\alpha,\beta,\gamma,\delta,\ldots}=\int_0^\infty dx\, e^{-x}L_\alpha(f_\alpha x)L_\beta(f_\beta x)L_\gamma(f_\gamma x)L_\delta(f_\delta x)\cdots , \tag{B1}$$

where the f_n's are known functions of the field frequencies. First, introduce a dummy variable μ such that each f_n is a function of μ. Now, take the derivative of Q with respect to μ and use the differential relation for Laguerre polynomials

$$\left[y\frac{d}{dy}L_m(y)=mL_m(y)-mL_{m-1}(y)\right]$$

to obtain

$$\frac{d}{d\mu}Q=\frac{f'_\alpha}{f_\alpha}\alpha(Q-Q_{\alpha-1})+\frac{f'_\beta}{f_\beta}\beta(Q-Q_{\beta-1})+\cdots , \tag{B2}$$

where $f'=df/d\mu$. Here the following shorthand notation has been introduced:

$$Q\equiv Q_{\alpha,\beta,\gamma,\delta,\ldots} ,$$

$$Q_{\alpha\pm1}\equiv Q_{\alpha\pm1,\beta,\gamma,\delta,\ldots} ,$$

$$Q_{\beta\pm1}\equiv Q_{\alpha,\beta\pm1,\gamma,\delta,\ldots} ,$$

etc. Next, make the change of variables $y=f_\alpha x$ so that Q becomes

$$Q_{\alpha,\beta,\gamma,\delta,\ldots}=\frac{1}{f_\alpha}\int_0^\infty dy\, e^{-y/f_\alpha}L_\alpha(y)L_\beta(yf_\beta/f_\alpha)\cdots . \tag{B3}$$

Again, take the derivative with respect to μ and use the Laguerre differential relation, as well as the Laguerre recursion relation,

$$yL_m(y)=-(m+1)L_{m+1}(y)+(2m+1)L_m(y)-mL_{m-1}(y) ,$$

to obtain

$$\begin{aligned}\frac{d}{d\mu}Q=&\frac{-f'_\alpha}{f_\alpha}Q-\frac{f'_\alpha}{f_\alpha^2}[(\alpha+1)Q_{\alpha+1}-(2\alpha+1)Q\\&+\alpha Q_{\alpha-1}]\\&+\left[\frac{f'_\beta}{f_\beta}-\frac{f'_\alpha}{f_\alpha}\right]\beta(Q-Q_{\beta-1})\\&+\left[\frac{f'_\gamma}{f_\gamma}-\frac{f'_\alpha}{f_\alpha}\right]\gamma(Q-Q_{\gamma-1})+\cdots .\end{aligned} \tag{B4}$$

Finally, by setting Eqs. (B2) and (B4) equal we obtain the recursion relation for Q with the index α changing:

$$(\alpha+1)Q_{\alpha+1}=(2\alpha+1)Q-\alpha Q_{\alpha-1}+f_\alpha K , \tag{B5a}$$

$$K=-(1+\alpha+\beta+\cdots)Q+\alpha Q_{\alpha-1}+\beta Q_{\beta-1}+\cdots . \tag{B5b}$$

Note that the explicit μ dependence of the f_n's is never required in the derivation. In fact, μ never has to be defined explicitly at all.

In general, the change of variables $y=f_n x$, $n=\alpha,\beta,\gamma,\delta,\ldots$ leads to the general formula

$$(n+1)Q_{n+1}=(2n+1)Q-nQ_{n-1}+f_n K . \tag{B6}$$

To use this set of recursion relations, we first require $Q_{n=-1}=Q_{-1,\beta,\gamma,\ldots}=Q_{\alpha,-1,\gamma,\ldots}=\cdots=0$. Then, with the initial value $Q_{000,\ldots}=\int_0^\infty dx\, e^{-x}=1$, all of the higher-order Q's may be evaluated.

If the problem under consideration is not rotationally symmetric, an expansion in Gauss-Hermite functions can be made. In this case, the coupling matrix will be a product of two integrals, one involving $H_\alpha(x)$'s and one involving $H_\beta(y)$'s. The above procedure to develop a recursion relation for the coupling matrix can then be applied to each of these integrals over Hermite polynomials.

[1]G. I. Kachen and W. H. Lowdermilk, Phys. Rev. A **16**, 1657 (1977).
[2]H. Gruhl and R. Sigel, IEEE J. Quant. Elect. **QE-20**, 1065 (1984).
[3]I. P. Cristov and I. V. Tomov, Opt. Quantum Electron. **17**, 207 (1985).
[4]B. Bobbs and C. Warner, Opt. Lett. **11**, 88 (1986).
[5]H. Kogelnik, Appl. Opt. **4**, 1562 (1965).
[6]A. A. Betin and G. A. Pasmanik, Kvant. Elektron. (Moscow) **4**, 60 (1973) [Sov. J. Quantum Electron. **3**, 312 (1974)].
[7]D. Cotter, D. C. Hanna, and R. Wyatt, Appl. Phys. **8**, 333 (1975).
[8]W. R. Trutna and R. L. Byer, Appl. Opt. **19**, 301 (1980).
[9]B. N. Perry, P. Rabinowitz, and M. Newstein, Phys. Rev. Lett.

49, 1921 (1982).
[10]B. N. Perry, P. Rabinowitz, and M. Newstein, Phys. Rev. A **27**, 1989 (1983).
[11]B. N. Perry, P. Rabinowitz, and D. S. Bomse, Opt. Lett. **10**, 146 (1985).
[12]M. S. Zubairy and J. K. McIver, Phys. Rev. A **31**, 856 (1985).
[13]A. Gavrielides and P. Peterson, J. Opt. Soc. Am. B **3**, 1394 (1986); P. R. Peterson, D. A. Cardimona, and A. Gavrielides, *ibid.* **4**, 1970 (1987).
[14]L. Allen and C. R. Stroud, Jr., Phys. Rep. **91**, 1 (1982).
[15]A. P. Hickman, J. A. Paisner, and W. K. Bischel, Phys. Rev. A **33**, 1788 (1986).
[16]P. Alsing, P. R. Peterson, D. A. Cardimona, and A. Gavrielides, IEEE J. Quantum Electron. **QE-23**, 557 (1987).
[17]A. Yariv, *Quantum Electronics* (Wiley, New York, 1975), pp. 110–113.
[18]W. K. Bischel and M. J. Dyer, Phys. Rev. A **33**, 3113 (1986).
[19]M. I. Baklushina, B. Ya. Zel'dovich, N. A. Mel'nikov, N. F. Pilipetskii, Yu. P. Raizer, A. N. Sudarkin, and V. V. Shkunov, Zh. Eksp. Teor. Fiz. **73**, 831 (1977) [Sov. Phys.—JETP **46**, 436 (1977)].
[20]W. M. Huo, G. C. Herring, and W. K. Bischel (unpublished).